Gravitation wave signal from asteroid mass primordial black hole dark matter

Diptimoy Ghosh* and Arvind Kumar Mishra†
Indian Institute of Science Education and Research, Pune 411008, India

(Received 7 May 2023; accepted 15 December 2023; published 29 February 2024)

Primordial black holes (PBHs) in the mass range $\sim 10^{17}$–10^{23} g are currently unconstrained, and can constitute the full dark matter (DM) density of the universe. Motivated by this, in the current work, we aim to relate the existence of PBHs in the said mass range to the production of observable gravitational waves (GWs) in the upcoming GW detectors. We follow a relatively model-independent approach assuming that the PBHs took birth in a radiation dominated era from enhanced primordial curvature perturbation at small scales produced by inflation. We show that the constraints from cosmic microwave background and BAO data allow for the possibility of PBHs being the whole of DM density of the universe. Finally, we derive the GW spectrum induced by the enhanced curvature perturbations and show that they are detectable in the future GW detectors like eLISA, LISA, BBO, and DECIGO.

DOI: 10.1103/PhysRevD.109.043537

I. INTRODUCTION

Primordial black holes (PBHs) are black holes which might have formed during the very early stages of the Universe [1–4]. There are various proposed mechanisms for the formation of these PBHs, and their masses can span a very large range of values, see Refs. [5–8] for recent reviews. Depending on the mass, PBHs can lead to different astrophysical and cosmological signatures which can be used to discover/constrain their existence. The PBHs have not been detected yet, but if they exist, they may contribute to dark matter (DM). For example, PBHs of mass $M_{\rm PBH} \leq 5 \times 10^{14}$ g are expected to have evaporated through Hawking radiation by now, and they cannot contribute to the dark matter density of the universe. Consequently, they do not produce astrophysical signatures, but may have effects on big bang nucleosynthesis (BBN) and/or cosmic microwave background (CMB) (see, for example, [9–14]). Heavier PBHs in the mass range 5×10^{14} g $\leq M_{\rm PBH} \leq 10^{17}$ g are evaporating at present and can be constrained from non-observation of Hawking emission products [15–20]. PBHs of mass more than 10^{22} g are constrained by gravitational lensing and other considerations, see for example, [5–7,21] and the references therein. However, PBHs in the intermediate mass range 10^{17}–10^{23} g (often refereed to as asteroid-mass PBHs) are very poorly constrained (for various efforts, see Refs. [22–32]). Therefore, in this mass range, PBHs can constitute the whole of DM, see Fig. 1.

PBHs can form due to enhanced primordial curvature perturbation at small scales produced by inflation in the very early Universe [1–3,33–35]. Since the scalar perturbations can give rise to also tensor modes at second order in perturbation theory, PBH production in this case inevitably leads to the scalar induced gravitational wave (SIGW) generation [36–56]. We estimate the SIGW spectrum corresponding to PBH DM mass in the range $\sim 10^{17}$–10^{23} g, and discuss the GW detection possibility using the upcoming GW detectors like eLISA, BBO and DECIGO. Note that, in the literature, PBH formation in the mass range of our interest has been studied in the context of specific inflationary models, for example, see Refs. [44,57–62]. In our work, we do not consider any specific inflationary model, but assume enhanced curvature power spectrum at small scales, see Sec. III for more details.

Our paper is organized as follows: In Sec. II, we briefly review the PBH formation, and associated secondary gravitational waves from enhanced scalar curvature perturbation. Section III describes the specific parametrization of power spectrum adopted for our analysis. Our main results are presented in Sec. IV. Finally, we summarize our findings in Sec. V.

II. PBH FORMATION AND SIGW GENERATION

In this section, we briefly review the primordial black hole formation and scalar induced gravitational wave generation. For a more detailed exposure see, Refs. [5–8,37,38,45,56,63].

*diptimoy.ghosh@iiserpune.ac.in
†arvind.mishra@acads.iiserpune.ac.in

Published by the American Physical Society under the terms of the Creative Commons Attribution 4.0 International license. Further distribution of this work must maintain attribution to the author(s) and the published article's title, journal citation, and DOI. Funded by SCOAP³.

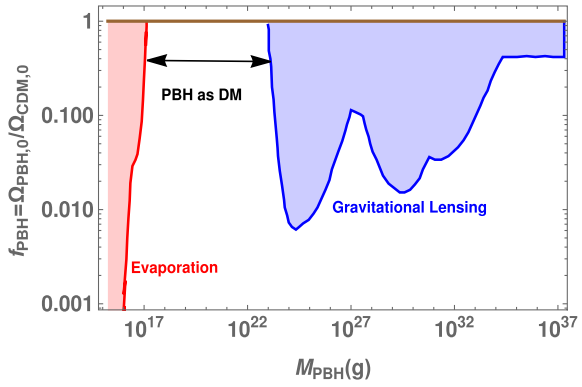

FIG. 1. The observational constraints on the PBH DM fraction, $f_{\rm PBH}$, for a monochromatic mass function for the PBH as a function of the PBH mass. The constraints are taken from [5].

A. Primordial black hole formation

As mentioned above, PBH formation can happen through various mechanisms, but here we focus on PBH generation via collapse of primordial density perturbation (produced during inflation) in a radiation-dominated era. In this mechanism, the PBHs form when a overdensity, δ, generated during inflation becomes larger than a critical density δ_c, re-enters into the horizon and collapses through gravitational instability [64]. The mass of the PBHs produced during the time when modes reenter into the horizon is assumed to be some fraction, γ, of the horizon mass at that epoch. The mass is therefore given by [65]

$$M_{\rm PBH}(k) = \gamma \frac{4\pi}{3} \rho H^{-3}\Big|_{k=aH}, \tag{1}$$

where ρ is the energy density, and a and H correspond to the scale factor and the Hubble expansion rate of the Universe respectively at the PBH formation epoch. Here $k = aH$ is the comoving scale of the mode associated with the density perturbation. In our calculations, we assume $\gamma = 0.2$ [4]. Since, in our study we study the PBH formation in a radiation-dominated era, all the above quantities are defined in the radiation era. So at the formation time, the PBHs mass is related to the comoving scale, k via

$$M_{\rm PBH}(k) \sim 5 \times 10^{15}\ {\rm g} \left(\frac{g_{\star,0}}{g_{\star,i}}\right)^{\frac{1}{6}} \left(\frac{10^{15}\ {\rm Mpc}^{-1}}{k}\right)^2 \tag{2}$$

where $g_{\star,0}$ and $g_{\star,i}$ are the relativistic degree of freedom associated with the energy density at present and PBH formation epoch. When PBH forms, its initial mass fraction, $\beta(M_{\rm PBH})$, is defined as

$$\beta(M_{\rm PBH}) = \frac{\rho_{{\rm PBH},i}}{\rho_{{\rm total},i}} \tag{3}$$

where $\rho_{{\rm PBH},i}$ and $\rho_{{\rm total},i}$ denote the energy densities of PBHs and the total energy density of the universe respectively at the time of PBH formation. Assuming, $\rho_{{\rm PBH},i} \propto a^{-3}$ and $\rho_{{\rm total},i} \propto a^{-4}$, we can rewrite $\beta(M_{\rm PBH})$ in terms of the present values of respective quantities as

$$\beta(M_{\rm PBH}) = \frac{\Omega_{{\rm PBH},0}(M_{\rm PBH})}{\Omega_{r,0}^{\frac{3}{4}}\gamma^{\frac{1}{2}}} \left(\frac{g_{\star,i}}{g_{\star,0}}\right)^{\frac{1}{4}} \left(\frac{M_{\rm PBH}}{M_{H0}}\right)^{\frac{1}{2}} \tag{4}$$

where $\Omega_{r,0} = \rho_{r,0}/\rho_{{\rm crit},0}$ is the ratio of present radiation energy density to the critical energy, $\rho_{{\rm crit},0}$ and $M_{H0} = \frac{4\pi}{3}\rho_{{\rm crit},0}H_0^{-3}$ is the present horizon mass.

The current density parameter for the PBHs which have not been evaporated yet is

$$\Omega_{{\rm PBH},0}(M_{\rm PBH}) = \frac{\rho_{{\rm PBH},0}(M_{\rm PBH})}{\rho_{{\rm crit},0}}. \tag{5}$$

where $\rho_{{\rm PBH},0}$ is the present PBH energy density. The quantity $f_{\rm PBH}$, defined as the fraction of current PBH mass density to the current cold dark matter (CDM) density is given by

$$f_{\rm PBH} = \frac{\Omega_{{\rm PBH},0}(M_{\rm PBH})}{\Omega_{{\rm CDM},0}}. \tag{6}$$

Using Eq. (4), (5), and (6), we obtain

$$f_{\rm PBH} = \frac{\beta(M_{\rm PBH})\Omega_{r,0}^{\frac{3}{4}}\gamma^{\frac{1}{2}}}{\Omega_{{\rm CDM},0}} \left(\frac{g_{\star,i}}{g_{\star,0}}\right)^{-\frac{1}{4}} \left(\frac{M_{\rm PBH}}{M_{H0}}\right)^{-\frac{1}{2}}. \tag{7}$$

The Press-Schechter theory [66] can now be used to obtain the expression of $\beta(M_{\rm PBH})$:

$$\beta(M_{\rm PBH}) = {\rm Erfc}\left(\frac{\delta_c}{\sqrt{2}\sigma(R)}\right), \tag{8}$$

where ${\rm Erfc}(y) = \frac{2}{\sqrt{\pi}}\int_y^\infty e^{-t^2}dt$ represent the complementary error function and δ_c is the critical value of density perturbation required for the PBH formation. A simple theoretical calculation gives $\delta_c = \frac{1}{3}$ [67] and numerical simulations obtained $\delta_c = 0.4$–45, see Refs. [68–70] and references therein. We take $\delta_c = 0.42$ for our calculations. Here $\sigma(R)$ is the mass variance which can be estimated at the horizon crossing via [71]

$$\sigma^2(R) = \int \tilde{W}^2(kR)\mathcal{P}_\delta(k)\frac{dk}{k} \tag{9}$$

where $P_\delta(k)$ and $\tilde{W}(kR)$ represent the matter power spectrum and the Fourier transform of the window function respectively. Here, w is equation of state of fluid, and is equal to $\frac{1}{3}$ for radiation-dominated epoch. In our calculation,

we consider a Gaussian window function, i.e., $\tilde{W}(kR) = \exp(-k^2R^2/2)$. The matter power spectrum, $P_\delta(k)$ is related to primordial curvature power spectrum $P_\mathcal{R}(k)$ by the relation

$$\mathcal{P}_\delta(k) = 4\left(\frac{1+w}{5+3w}\right)^2 \mathcal{P}_\mathcal{R}(k) \tag{10}$$

where $P_\mathcal{R}(k)$ is defined as

$$\langle \mathcal{R}(k)\mathcal{R}(k')\rangle = \frac{2\pi^2}{k^3}\delta^3(\mathbf{k}+\mathbf{k}')\mathcal{P}_\mathcal{R}(k). \tag{11}$$

Here $\mathcal{R}(k)$ is the primordial curvature perturbation. Therefore, using Eq. (10), Eq. (9), and Eq. (8) in Eq. (7), we can calculate the PBH dark matter fraction, $f_{\rm PBH}$, as a function of PBH mass.

We have used $h^2\Omega_{\rm CDM,0} = 0.11933$, $h^2\Omega_{\rm B,0} = 0.02242$, and $h = 0.6766$ [72] in our numerical computations.

B. Scalar induced gravitational waves

The scalar modes couple to the tensor modes at the second order in perturbation theory. At the time of PBH formation, the scalar perturbations are enhanced giving rise to the possibility of significant second order tensor perturbations. Thus, PBH production indirectly induce gravitational waves [36–39]. The fraction of GW energy density per logarithmic k interval to the total energy density is given by [38,45]

$$\Omega_{\rm GW}(\eta,k) = \frac{1}{24}\left(\frac{\rm k}{a(\eta)H(\eta)}\right)^2 \overline{\mathcal{P}_h(\eta,{\rm k})} \tag{12}$$

where, $\mathcal{P}_h(\eta,{\rm k})$ is the dimensionless power spectrum of tensor perturbation, defined via

$$\langle h^\lambda_{\mathbf{k}}(\eta) h^{\lambda'}_{\mathbf{k}'}(\eta)\rangle = \frac{2\pi^2}{k^3}\delta_{\lambda\lambda'}\delta^3(\mathbf{k}+\mathbf{k}')\mathcal{P}_h(\eta,k). \tag{13}$$

Here $h^\lambda_{\mathbf{k}}(\eta)$ is the Fourier decomposition of tensor metric perturbations and, $\lambda,\lambda' = +,\times$ corresponds to the polarization index. Further, overbar on tensor power spectrum, i.e., $\overline{\mathcal{P}_h(\eta,{\rm k})}$ represent averaged over time. Assuming vanishing anisotropic stress and neglecting the non-Gaussianity in the primordial curvature power spectrum, we obtain the tensor power spectrum as [38,45]

$$\mathcal{P}_h(\eta,k) = 4\int_0^\infty dv \int_{|1-v|}^{|1+v|} du \left[\frac{4v^2-(1+v^2-u^2)^2}{4vu}\right]^2 \times [{\rm I}(v,u,x)]^2 P_\mathcal{R}(kv)P_\mathcal{R}(ku) \tag{14}$$

where $u = |\mathbf{k}-\tilde{\mathbf{k}}|/{\rm k}$ and $v = \tilde{\rm k}/{\rm k}$ are dimensionless variables. In the above equation, $x \equiv k\eta$ and the function ${\rm I}(v,u,x)$ is defined in Ref. [45]. Using Eq. (12), the energy spectrum of induced gravitational waves $\Omega_{\rm GW,0}(k)$ at the present time can be obtained [73]:

$$\Omega_{\rm GW,0}(k) = 0.39\left(\frac{g_\star}{106.75}\right)^{-\frac{1}{3}}\Omega_{r,0}\Omega_{\rm GW}(\eta_c,k) \tag{15}$$

where η_c is the conformal time when a perturbation is inside the horizon during radiation dominated era. In the above equation, $\Omega_{r,0} \approx 9\times10^{-5}$ is the present radiation energy density, and $g_\star$ is the effective number of relativistic degree of freedom in the radiation dominated era. To calculate the gravitational wave energy density, $\Omega_{\rm GW,0}$, as a function of frequency, we express k in terms of frequency, f, using

$$f = \frac{k}{2\pi} = 1.5\times10^{-15}\left(\frac{k}{1\ {\rm Mpc}^{-1}}\right)\ {\rm Hz}. \tag{16}$$

III. PARAMETRIZATION OF PRIMORDIAL CURVATURE PERTURBATIONS

Amplitude of the power spectrum at large scales $k \sim 0.05\ {\rm Mpc}^{-1}$ is measured from CMB to be $P_\mathcal{R} = 2.1\times10^{-9}$ [74]. PBHs formation (with appreciable amount) at small scales however requires much larger amplitude, $P_\mathcal{R}(k) \sim \mathcal{O}(10^{-2})$. Therefore, scale-invariant, $n_s = 1$ and red-tilted, $n_s < 1$ power spectrum will not be able to form PBHs. In order to form sufficient PBH abundance, the curvature power spectrum needs to be enhanced by several orders of magnitudes at small scales. This suggests one to explore some possible physical mechanisms to increase the primordial power spectrum in the early universe. In this work, following Ref. [75], we assume a phenomenological form of curvature power spectrum parametrized by the scalar spectral index, it's running and also its running of running:

$$\mathcal{P}_\mathcal{R}(k) = A_s\left(\frac{k}{k_p}\right)^{n_s-1+\frac{\alpha_s}{2}\log(\frac{k}{k_p})+\frac{\beta_s}{6}(\log(\frac{k}{k_p}))^2}, \tag{17}$$

where $k_p = 0.05\ {\rm Mpc}^{-1}$ is the pivot scale. Here, n_s, $\alpha_s \equiv dn_s/d\ln k$ and $\beta_s \equiv d^2n_s/d\ln k^2$ correspond to scalar spectral index, it's running and also it's running of running. This kind of parametrization has also been discussed earlier in the literature [76–78]. For positive values of running parameters, i.e., $\alpha_s > 0, \beta_s > 0$, $\mathcal{P}_\mathcal{R}(k)$ can be enhanced at large k, and can, in principle, lead to PBH formation. Nevertheless depending on the positive values of α_s, and β_s, $\mathcal{P}_\mathcal{R}(k) \sim 10^{-2}$ on different k values. From Eq. (2), it is also clear that larger (smaller) k will produce smaller (larger) mass PBHs.

For our estimation, we consider α_s and β_s values obtained from Planck and BAO data [75] (see also, [77])

$$\ln(10^{10}A_s) = 3.088 \pm 0.023, \quad n_s = 0.9660 \pm 0.0040,$$
$$\alpha_s = 0.0077^{+0.0104}_{-0.0103}, \quad \beta_s = 0.019 \pm 0.013. \tag{18}$$

In the light of the constraints on α_s and β_s parameter, we check the PBH formation in this model. Assuming, $A_s = 2.19 \times 10^{-9}$, $n_s = 0.9660$, and using Eq. (17), PBH formation with sufficient abundance at scale k, i.e., $P_{\mathcal{R}}(k) \sim \mathcal{O}(10^{-2})$ suggests,

$$(20k)^{-0.034+\frac{\alpha_s}{2}\log(20k)+\frac{\beta_s}{6}(\log(20k))^2} \sim 4.56 \times 10^6. \tag{19}$$

It is evident that there is a degeneracy between α_s and β_s parameters for PBH formation at some scale k. Nevertheless, for a fixed values of A_s and n_s, comparable to α_s, the enhancement of power spectrum is more sensitive to β_s parameter. Note that the α_s and β_s parameters are related to higher order slow-roll parameters [75]; therefore they can in principle tell us about the inflationary models [79]. PBH formation in the context of an enhanced power spectrum has also been discussed in [64,70,80,81].

IV. RESULTS AND DISCUSSIONS

Following the basic formalism of PBH formation and the parametrization of the curvature power spectrum, we can now discuss the PBH production in the mass range $\sim 10^{17}$ g–10^{23} g constituting the whole of DM density. We consider that the PBHs in the aforementioned mass range form when the corresponding modes reenter the horizon after inflation during a radiation-dominated era.

Before discussing the PBH formation, let us first show the primordial curvature power spectrum as a function of k for different set of values of α_s and β_s in Fig. 2. The magenta (0.008262,0.0017), purple (0.0083,0.00193), black (0.00873,0.00216), and cyan (0.00844,0.0025) curves correspond to four benchmark values of α_s, β_s. The values of model parameters are quite arbitrary, but these are required to get the correct energy density of dark matter at a very specific PBH mass. We may adopt some different choices, but using those choices, we will be unable to show the peak of DM fraction on the specific mass we are interested in; please see Fig. 3. Further, it is clear from Fig. 2 that $\mathcal{P}_{\mathcal{R}}(k)$ corresponding to benchmark values are consistent with the Planck measurement at small k but the amplitude grows sharply to $\mathcal{P}_{\mathcal{R}}(k) \sim \mathcal{O}(10^{-2})$ at large k allowing the formation of PBHs. The brown-dashed line corresponds to the power spectrum with $\alpha_s = 0$, $\beta_s = 0$. Note that all the lines are consistent with the Planck measurement at small k. In the case of $\alpha_s = 0$, $\beta_s = 0$, the spectral index is red, i.e., $n_s < 1$, and $\mathcal{P}_{\mathcal{R}}(k)$ decreases with increasing k (thus being unable to produce PBHs).

Figure 3 shows the PBH fraction, $f_{\rm PBH}$, as a function of the PBH mass, $M_{\rm PBH}$ corresponding to the (α_s, β_s) values considered earlier. The existing constraints on the PBH fraction as DM are also superimposed. Here, we see that every model of the power spectrum, $P(k)$ (i.e., each choice of alpha, beta), leads to a mass spectrum. For fixed values of parameters, $(\alpha_s$, and $\beta_s)$, $f_{\rm PBH}$ increases as mass decreases. This is because $f_{\rm PBH}$ depends on $\mathcal{P}_{\mathcal{R}}(k)$ via $\beta(M_{\rm PBH})$ and $(M_{\rm PBH})^{-1/2}$ [see, Eq. (7)]. It is clear that enhancement in $\mathcal{P}_{\mathcal{R}}(k)$ causes to increases $\beta(M_{\rm PBH})$ and hence $f_{\rm PBH}$. For large power spectrum, i.e., $P_{\mathcal{R}}(k) \sim \mathcal{O}(10^{-2})$, $f_{\rm PBH} \sim 1$ and therefore PBHs can be full dark matter. The magenta, purple, black, and cyan curves show that $f_{\rm PBH} = 1$ can indeed be obtained in the asteroid mass region, for example, for the PBH masses 10^{18} g, 10^{19} g, 10^{20} g, and 10^{21} g respectively.

In Fig. 4 we plot the present GW energy density as a function of the frequency again for the same four set of benchmark values of α_s, β_s. The sensitivity curves for the present and future GW detectors are taken from [45,83–88]. The constraint on the GW background from BBN, i.e., $\Omega_{\rm GW,0}h^2 < 5 \times 10^{-6}$ is taken from [83,89]. From Eq. (12) and Eq. (14), one can see that the GW energy density depends on the behavior of the primordial power spectrum. In our case, $\mathcal{P}_{\mathcal{R}}(k)$ is increasing with scale k; therefore,

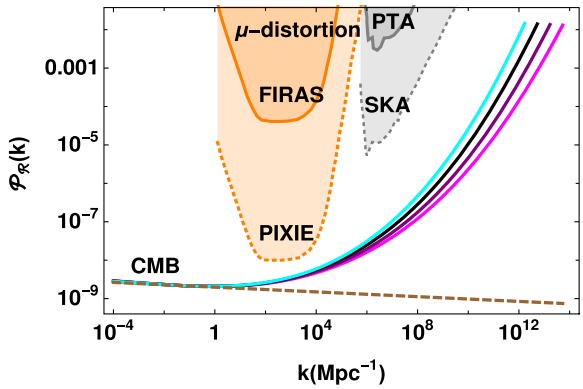

FIG. 2. The primordial curvature power spectrum as a function of the scale k for different set of values of α_s and β_s. The constraints on $\mathcal{P}_{\mathcal{R}}(k)$ from μ − distortion, PTA and SKA are also shown [82].

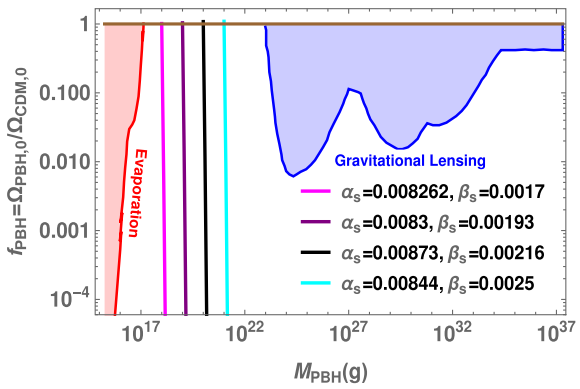

FIG. 3. The PBH fraction, $f_{\rm PBH}$, corresponding to four set of benchmark values of α_s, β_s showing that the PBHs can indeed be the whole of DM in the asteroid mass region. The constraints on $f_{\rm PBH}$ from evaporation and gravitational lensing [5] are also shown.

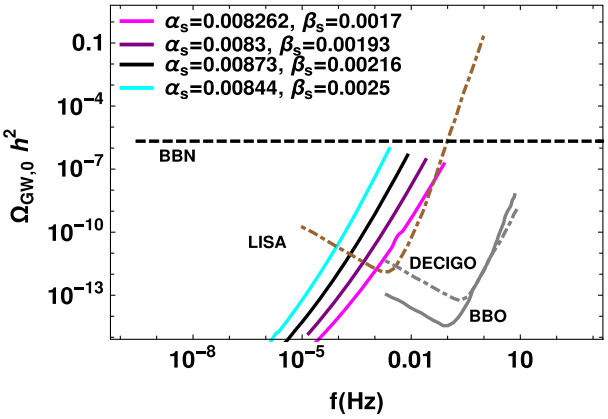

FIG. 4. The scalar induced GW energy density as a function of the frequency for the four benchmark parameter sets. Sensitivity curves of some of the future GW detectors are also shown for comparison.

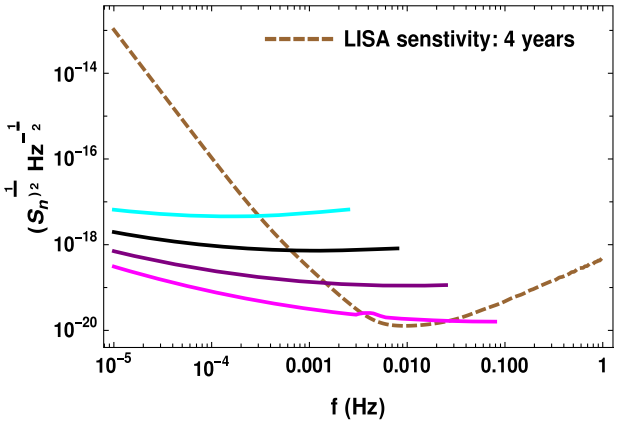

FIG. 5. The sensitivity curve (for 4 years) for the LISA mission along with the SIGW prediction for the four benchmark parameter sets. The plot of spectral sensitivity, S_n for the LISA is taken from Ref. [86].

GW energy density will increase accordingly. As we are exploring the primordial black hole dark matter formation in the asteroid mass range, the curves should increase and should be saturated at the scale for which PBHs can contribute to the full dark matter abundance, i.e., $f_{\rm PBH} = 1$. Further, the primordial power spectrum must be suppressed beyond this scale as the behavior of the power spectrum has been strongly constrained by the various observations, see Ref. [7]. To control the strength of the primordial power spectrum theoretically, various mechanisms are possible which crucially depend on the models of inflationary potentials. In these models, firstly the power spectrum increases and after some scale, it starts decreasing, for example in potential with ultraslow roll condition power spectrum decreases as the ultraslow roll phase ends [90] (see also a warm inflation model [73]). Further in some other model such as the sharp cutoff model, the power spectrum sharply decreases after some value of the power spectrum due to the end of inflation, please see Ref. [70]. In our case, the primordial power spectrum is model-independent ($\mathcal{P}_\mathcal{R}(k)$ is parametrized by n_s, α_s and β_s); therefore, we have not used any suppression mechanism in the estimation. However, in our analysis, a sharp cutoff or power law cutoff in the $\mathcal{P}_\mathcal{R}(k)$ can be used as given in Ref. [70]. In this work, for simplicity, we have restricted our analysis to scale, leading to $f_{\rm PBH} = 1$.

One can see from Fig. 4 that the peak GW frequency lies in the range: 10^{-3} Hz–10^{-1} Hz. So the sensitivity curves suggest that the GWs can be detected by future detectors like LISA, BBO and DECIGO. As we can see, the SIGW signal can be detected mostly in the LISA mission. Therefore, following Refs. [91,92], we plot the LISA sensitivity curve for the same four sets of benchmark values of α_s, β_s in Fig. 5. To plot the LISA sensitivity curves (for 4 years), we follow Ref. [86]. It is reflected from Fig. 5 that the 4 years of LISA observation is sufficient to detect the SIGW produced during the PBH formation in our model.

V. SUMMARY

PBHs in the asteroid mass window 10^{17}–10^{23} g are currently unconstrained to constitute the whole of DM density of our universe. In this paper, we explore the possibility of formation of PBHs in this mass range considering a phenomenological parametrization (in terms of two parameters α_s and β_s) of an enhanced curvature power spectrum. Using allowed values of α_s and β_s from the Plank and BAO data, we have shown that one can indeed get full PBH DM abundance in the said mass range.

Using the same set of α_s and β_s parameters, we also calculated the scalar induced GW spectrum and showed that they fall in the sensitivity region of future GW detectors like LISA, BBO, and DECIGO.

Further, sensitivity curves of GW signal generated in our model (as indirect evidence of large PBH abundance in the asteroid mass region) suggest some characteristic features that can be used to distinguish it from GWs generated by other mechanisms, e.g., astrophysical sources [93,94]. Therefore, detecting such a gravitational wave will shed light on the physics of the early universe. It would also be interesting to check what kind of inflationary models can produce such a large power spectrum at small scales required for significant PBH production. We leave these questions for future work.

ACKNOWLEDGMENTS

D. G. and A. K. M. acknowledge support through the Ramanujan Fellowship and MATRICS Grant of the Department of Science and Technology, Government of India. We thank Arka Banerjee and Susmita Adhikari for valuable comments. A. K. M. would also like to thank Richa Arya for fruitful suggestions and helping in the *Mathematica* program.

[1] Y. B. Zel'dovich and I. D. Novikov, The hypothesis of cores retarded during expansion and the hot cosmological model, Sov. Astron. **10**, 602 (1967).

[2] S. Hawking, Gravitationally collapsed objects of very low mass, Mon. Not. R. Astron. Soc. **152**, 75 (1971).

[3] B. J. Carr and S. W. Hawking, Black holes in the early universe, Mon. Not. R. Astron. Soc. **168**, 399 (1974).

[4] B. J. Carr, The primordial black hole mass spectrum, Astrophys. J. **201**, 1 (1975).

[5] B. Carr and F. Kuhnel, Primordial black holes as dark matter: Recent developments, Annu. Rev. Nucl. Part. Sci. **70**, 355 (2020).

[6] A. M. Green and B. J. Kavanagh, Primordial black holes as a dark matter candidate, J. Phys. G **48**, 043001 (2021).

[7] B. Carr and F. Kuhnel, Primordial black holes as dark matter candidates, SciPost Phys. Lect. Notes **48**, 1 (2022).

[8] S. Bird *et al.*, Snowmass2021 Cosmic Frontier White Paper: Primordial black hole dark matter, Phys. Dark Universe **41**, 101231 (2023).

[9] B. V. Vainer and P. D. Naselskii, Observable consequences of the evaporation of low-mass primordial black holes, Sov. Astron. Lett. **3**, 76 (1977).

[10] I. B. Zeldovich, A. A. Starobinskii, M. I. Khlopov, and V. M. Chechetkin, Primordial black holes and the deuterium problem, Sov. Astron. Lett. **3**, 110 (1977).

[11] K. Kohri and J. Yokoyama, Primordial black holes and primordial nucleosynthesis. 1. Effects of hadron injection from low mass holes, Phys. Rev. D **61**, 023501 (2000).

[12] B. J. Carr, K. Kohri, Y. Sendouda, and J. Yokoyama, New cosmological constraints on primordial black holes, Phys. Rev. D **81**, 104019 (2010).

[13] S. K. Acharya and R. Khatri, CMB and BBN constraints on evaporating primordial black holes revisited, J. Cosmol. Astropart. Phys. 06 (2020) 018.

[14] J. Chluba, A. Ravenni, and S. K. Acharya, Thermalization of large energy release in the early Universe, Mon. Not. R. Astron. Soc. **498**, 959 (2020).

[15] M. Boudaud and M. Cirelli, Voyager 1 $e^{\pm}$ further constrain primordial black holes as dark matter, Phys. Rev. Lett. **122**, 041104 (2019).

[16] R. Laha, Primordial black holes as a dark matter candidate are severely constrained by the galactic center 511 keV γ -ray line, Phys. Rev. Lett. **123**, 251101 (2019).

[17] W. DeRocco and P. W. Graham, Constraining primordial black hole abundance with the galactic 511 keV line, Phys. Rev. Lett. **123**, 251102 (2019).

[18] K. M. Belotsky and A. A. Kirillov, Primordial black holes with mass 10^{16}–10^{17} g and reionization of the Universe, J. Cosmol. Astropart. Phys. 01 (**2015**) 041.

[19] M. H. Chan and C. M. Lee, Constraining primordial black hole fraction at the galactic centre using radio observational data, Mon. Not. R. Astron. Soc. **497**, 1212 (2020).

[20] R. Laha, J. B. Muñoz, and T. R. Slatyer, INTEGRAL constraints on primordial black holes and particle dark matter, Phys. Rev. D **101**, 123514 (2020).

[21] B. Carr, K. Kohri, Y. Sendouda, and J. Yokoyama, Constraints on primordial black holes, Rep. Prog. Phys. **84**, 116902 (2021).

[22] F. Capela, M. Pshirkov, and P. Tinyakov, Constraints on primordial black holes as dark matter candidates from star formation, Phys. Rev. D **87**, 023507 (2013).

[23] F. Capela, M. Pshirkov, and P. Tinyakov, Constraints on primordial black holes as dark matter candidates from capture by neutron stars, Phys. Rev. D **87**, 123524 (2013).

[24] P. Pani and A. Loeb, Tidal capture of a primordial black hole by a neutron star: Implications for constraints on dark matter, J. Cosmol. Astropart. Phys. 06 (2014) 026.

[25] B. Dasgupta, R. Laha, and A. Ray, Neutrino and positron constraints on spinning primordial black hole dark matter, Phys. Rev. Lett. **125**, 101101 (2020).

[26] S. Mittal, A. Ray, G. Kulkarni, and B. Dasgupta, Constraining primordial black holes as dark matter using the global 21-cm signal with X-ray heating and excess radio background, J. Cosmol. Astropart. Phys. 03 (2022) 030.

[27] D. Ghosh, D. Sachdeva, and P. Singh, Future constraints on primordial black holes from XGIS-THESEUS, Phys. Rev. D **106**, 023022 (2022).

[28] A. Katz, J. Kopp, S. Sibiryakov, and W. Xue, Femtolensing by dark matter revisited, J. Cosmol. Astropart. Phys. 12 (2018) 005.

[29] P. Montero-Camacho, X. Fang, G. Vasquez, M. Silva, and C. M. Hirata, Revisiting constraints on asteroid-mass primordial black holes as dark matter candidates, J. Cosmol. Astropart. Phys. 08 (2019) 031.

[30] N. Esser and P. Tinyakov, Constraints on primordial black holes from observation of stars in dwarf galaxies, Phys. Rev. D **107**, 103052 (2023).

[31] A. Ray, R. Laha, J. B. Muñoz, and R. Caputo, Near future MeV telescopes can discover asteroid-mass primordial black hole dark matter, Phys. Rev. D **104**, 023516 (2021).

[32] P. K. Natwariya, A. C. Nayak, and T. Srivastava, Constraining spinning primordial black holes with global 21-cm signal, Mon. Not. R. Astron. Soc. **510**, 4236 (2021).

[33] S. W. Hawking, I. G. Moss, and J. M. Stewart, Bubble collisions in the very early universe, Phys. Rev. D **26**, 2681 (1982).

[34] C. J. Hogan, Massive black holes generated by cosmic strings, Phys. Lett. **143B**, 87 (1984).

[35] S. W. Hawking, Black holes from cosmic strings, Phys. Lett. B **231**, 237 (1989).

[36] S. Mollerach, D. Harari, and S. Matarrese, CMB polarization from secondary vector and tensor modes, Phys. Rev. D **69**, 063002 (2004).

[37] K. N. Ananda, C. Clarkson, and D. Wands, The cosmological gravitational wave background from primordial density perturbations, Phys. Rev. D **75**, 123518 (2007).

[38] D. Baumann, P. J. Steinhardt, K. Takahashi, and K. Ichiki, Gravitational wave spectrum induced by primordial scalar perturbations, Phys. Rev. D **76**, 084019 (2007).

[39] R. Saito and J. Yokoyama, Gravitational wave background as a probe of the primordial black hole abundance, Phys. Rev. Lett. **102**, 161101 (2009); **107**, 069901(E) (2011).

[40] E. Bugaev and P. Klimai, Induced gravitational wave background and primordial black holes, Phys. Rev. D **81**, 023517 (2010).

[41] L. Alabidi, K. Kohri, M. Sasaki, and Y. Sendouda, Observable spectra of induced gravitational waves from inflation, J. Cosmol. Astropart. Phys. 09 (**2012**) 017.

[42] K. Inomata, M. Kawasaki, K. Mukaida, and T. T. Yanagida, Double inflation as a single origin of primordial black holes for all dark matter and LIGO observations, Phys. Rev. D **97**, 043514 (2018).
[43] N. Orlofsky, A. Pierce, and J. D. Wells, Inflationary theory and pulsar timing investigations of primordial black holes and gravitational waves, Phys. Rev. D **95**, 063518 (2017).
[44] W. Ahmed, M. Junaid, and U. Zubair, Primordial black holes and gravitational waves in hybrid inflation with chaotic potentials, Nucl. Phys. **B984**, 115968 (2022).
[45] K. Kohri and T. Terada, Semianalytic calculation of gravitational wave spectrum nonlinearly induced from primordial curvature perturbations, Phys. Rev. D **97**, 123532 (2018).
[46] C. Fu, P. Wu, and H. Yu, Scalar induced gravitational waves in inflation with gravitationally enhanced friction, Phys. Rev. D **101**, 023529 (2020).
[47] Q. Gao, Primordial black holes and secondary gravitational waves from chaotic inflation, Sci. China Phys. Mech. Astron. **64**, 280411 (2021).
[48] Z. Yi, Q. Gao, Y. Gong, and Z.-h. Zhu, Primordial black holes and scalar-induced secondary gravitational waves from inflationary models with a noncanonical kinetic term, Phys. Rev. D **103**, 063534 (2021).
[49] J. Lin, S. Gao, Y. Gong, Y. Lu, Z. Wang, and F. Zhang, Primordial black holes and scalar induced secondary gravitational waves from Higgs inflation with non-canonical kinetic term, Phys. Rev. D **107**, 043517 (2023).
[50] N. Bhaumik and R. K. Jain, Small scale induced gravitational waves from primordial black holes, a stringent lower mass bound, and the imprints of an early matter to radiation transition, Phys. Rev. D **104**, 023531 (2021).
[51] H. V. Ragavendra, P. Saha, L. Sriramkumar, and J. Silk, Primordial black holes and secondary gravitational waves from ultraslow roll and punctuated inflation, Phys. Rev. D **103**, 083510 (2021).
[52] J. Lin, Q. Gao, Y. Gong, Y. Lu, C. Zhang, and F. Zhang, Primordial black holes and secondary gravitational waves from k and G inflation, Phys. Rev. D **101**, 103515 (2020).
[53] J.-Z. Zhou, X. Zhang, Q.-H. Zhu, and Z. Chang, The third order scalar induced gravitational waves, J. Cosmol. Astropart. Phys. 05 (2022) 013.
[54] G. Domènech, Scalar induced gravitational waves review, Universe **7**, 398 (2021).
[55] S. Balaji, J. Silk, and Y.-P. Wu, Induced gravitational waves from the cosmic coincidence, J. Cosmol. Astropart. Phys. 06 (2022) 008.
[56] R. Arya and A. K. Mishra, Scalar induced gravitational waves from warm inflation, Phys. Dark Universe **37**, 101116 (2022).
[57] N. Bartolo, V. De Luca, G. Franciolini, M. Peloso, D. Racco, and A. Riotto, Testing primordial black holes as dark matter with LISA, Phys. Rev. D **99**, 103521 (2019).
[58] N. Bartolo, V. De Luca, G. Franciolini, A. Lewis, M. Peloso, and A. Riotto, Primordial black hole dark matter: LISA serendipity, Phys. Rev. Lett. **122**, 211301 (2019).
[59] M. Braglia, D. K. Hazra, F. Finelli, G. F. Smoot, L. Sriramkumar, and A. A. Starobinsky, Generating PBHs and small-scale GWs in two-field models of inflation, J. Cosmol. Astropart. Phys. 08 (**2020**) 001.
[60] S. Kawai and J. Kim, Primordial black holes from Gauss-Bonnet-corrected single field inflation, Phys. Rev. D **104**, 083545 (2021).
[61] V. C. Spanos and I. D. Stamou, Gravitational waves and primordial black holes from supersymmetric hybrid inflation, Phys. Rev. D **104**, 123537 (2021).
[62] M. Correa, M. R. Gangopadhyay, N. Jaman, and G. J. Mathews, Primordial black-hole dark matter via warm natural inflation, Phys. Lett. B **835**, 137510 (2022).
[63] R. Arya, Formation of primordial black holes from warm inflation, J. Cosmol. Astropart. Phys. 09 (2020) 042.
[64] M. Sasaki, T. Suyama, T. Tanaka, and S. Yokoyama, Primordial black holes—perspectives in gravitational wave astronomy, Classical Quantum Gravity **35**, 063001 (2018).
[65] A. M. Green and A. R. Liddle, Constraints on the density perturbation spectrum from primordial black holes, Phys. Rev. D **56**, 6166 (1997).
[66] W. H. Press and P. Schechter, Formation of galaxies and clusters of galaxies by self-similar gravitational condensation, Astrophys. J. **187**, 425 (1974).
[67] B. J. Carr, The primordial black hole mass spectrum., Astrophys. J. **201**, 1 (1975).
[68] T. Harada, C.-M. Yoo, and K. Kohri, Threshold of primordial black hole formation, Phys. Rev. D **88**, 084051 (2013); **89**, 029903(E) (2014).
[69] T. Harada, C.-M. Yoo, T. Nakama, and Y. Koga, Cosmological long-wavelength solutions and primordial black hole formation, Phys. Rev. D **91**, 084057 (2015).
[70] K. Kohri and T. Terada, Primordial black hole dark matter and LIGO/Virgo merger rate from inflation with running spectral indices: Formation in the matter- and/or radiation-dominated universe, Classical Quantum Gravity **35**, 235017 (2018).
[71] A. R. Liddle and D. H. Lyth, Cosmological Inflation and Large-Scale Structure (2000), https://ui.adsabs.harvard.edu/abs/2000cils.book.....L.
[72] N. Aghanim *et al.* (Planck Collaboration), Planck 2018 results. VI. Cosmological parameters, Astron. Astrophys. **641**, A6 (2020); **652**, C4(E) (2021).
[73] M. Bastero-Gil and M. S. Díaz-Blanco, Gravity waves and primordial black holes in scalar warm little inflation, J. Cosmol. Astropart. Phys. 12 (2021) 052.
[74] Y. Akrami *et al.* (Planck Collaboration), Planck 2018 results. X. Constraints on inflation, arXiv:1807.06211.
[75] J. Li and Q.-G. Huang, Measuring the spectral running from cosmic microwave background and primordial black holes, Eur. Phys. J. C **78**, 980 (2018).
[76] A. Kosowsky and M. S. Turner, CBR anisotropy and the running of the scalar spectral index, Phys. Rev. D **52**, R1739 (1995).
[77] Y. Akrami *et al.* (Planck Collaboration), Planck 2018 results. X. Constraints on inflation, Astron. Astrophys. **641**, A10 (2020).
[78] A. M. Green, Pitfalls of a power-law parametrization of the primordial power spectrum for primordial black hole formation, Phys. Rev. D **98**, 023529 (2018).
[79] M. Drees and E. Erfani, Running spectral index and formation of primordial black hole in single field inflation models, J. Cosmol. Astropart. Phys. 01 (2012) 035.

[80] A. S. Josan, A. M. Green, and K. A. Malik, Generalised constraints on the curvature perturbation from primordial black holes, Phys. Rev. D **79**, 103520 (2009).
[81] M. Drees and E. Erfani, Running-mass inflation model and primordial black holes, J. Cosmol. Astropart. Phys. 04 (2011) 005.
[82] J. Chluba *et al.*, Spectral distortions of the CMB as a probe of inflation, recombination, structure formation and particle physics: Astro2020 Science White Paper, Bull. Am. Astron. Soc. **51**, 184 (2019).
[83] M. Maggiore, Gravitational wave experiments and early universe cosmology, Phys. Rep. **331**, 283 (2000).
[84] H. Assadullahi and D. Wands, Constraints on primordial density perturbations from induced gravitational waves, Phys. Rev. D **81**, 023527 (2010).
[85] B. P. Abbott *et al.*, An upper limit on the stochastic gravitational-wave background of cosmological origin, Nature (London) **460**, 990 (2009).
[86] C. J. Moore, R. H. Cole, and C. P. L. Berry, Gravitational-wave sensitivity curves, Classical Quantum Gravity **32**, 015014 (2015).
[87] K. Inomata and T. Nakama, Gravitational waves induced by scalar perturbations as probes of the small-scale primordial spectrum, Phys. Rev. D **99**, 043511 (2019).
[88] V. Mandic and E. Floden, GW plotter webpage, https://homepages.spa.umn.edu/gwplotter.
[89] B. Abbott *et al.* (LIGO Scientific Collaboration), Searching for a stochastic background of gravitational waves with LIGO, Astrophys. J. **659**, 918 (2007).
[90] G. Ballesteros and M. Taoso, Primordial black hole dark matter from single field inflation, Phys. Rev. D **97**, 023501 (2018).
[91] T. Robson, N. J. Cornish, and C. Liu, The construction and use of LISA sensitivity curves, Classical Quantum Gravity **36**, 105011 (2019).
[92] S. Babak, A. Petiteau, and M. Hewitson, LISA sensitivity and SNR calculations, arXiv:2108.01167.
[93] P. A. Seoane *et al.* (LISA Collaboration), Astrophysics with the Laser Interferometer Space Antenna, Living Rev. Relativity **26**, 2 (2023).
[94] P. Auclair *et al.* (LISA Cosmology Working Group Collaboration), Cosmology with the Laser Interferometer Space Antenna, Living Rev. Relativity **26**, 5 (2023).